Impact of solar-induced stratospheric ozone decline on Southern Hemisphere westerlies during the Late Maunder Minimum

V. Varma,[1] M. Prange,[1,2] T. Spangehl,[3,4] F. Lamy,[1,5] U. Cubasch,[3] and M. Schulz[1,2]

Received 31 July 2012; revised 10 September 2012; accepted 16 September 2012; published 19 October 2012.

[1] The Southern Hemisphere Westerly Winds (SWW) constitute an important zonal circulation system that dominates the dynamics of the Southern Hemisphere mid-latitudes. In the present study, we analyze results from two transient simulations (1630–2000 AD) conducted with the coupled atmosphere-ocean model EGMAM (ECHO-G with Middle Atmosphere Model): one simulation with fixed stratospheric ozone concentration, and one with solar-induced variations in stratospheric ozone content. The results suggest that during periods of lower solar activity, the annual-mean SWW tend to get weaker on their poleward side and shift towards the equator. The SWW shift is more intense and robust for the simulation with varying stratospheric ozone, suggesting an important influence of solar-induced stratospheric ozone variations on mid-latitude troposphere dynamics. Finally, we present proxy evidence from a high-resolution marine sediment core from the Chilean continental slope (41°S), which strongly supports the model result of an equatorward displacement of the SWW during the Maunder Minimum.
Citation: Varma, V., M. Prange, T. Spangehl, F. Lamy, U. Cubasch, and M. Schulz (2012), Impact of solar-induced stratospheric ozone decline on Southern Hemisphere westerlies during the Late Maunder Minimum, *Geophys. Res. Lett.*, *39*, L20704, doi:10.1029/2012GL053403.

1. Introduction

[2] The Southern Hemisphere Westerly Winds (SWW) constitute an important zonal circulation system that dominates the dynamics of Southern Hemisphere (SH) mid-latitude climate, influencing large-scale precipitation patterns and atmospheric heat transports [e.g., *Shulmeister et al.*, 2004]. Furthermore, they may influence the global ocean circulation [e.g., *Toggweiler and Samuels*, 1995; *Biastoch et al.*, 2009] as well as the CO_2 budget in the Southern Ocean [*Toggweiler et al.*, 2006; *Anderson et al.*, 2009]. Thus, understanding the forcings and mechanisms behind SWW variability remains a significant area of research.

[3] Solar variations - in terms of total solar irradiance (TSI) - have recently been suggested to be a potential driver for centennial-scale SWW variability [*Varma et al.*, 2011]. A 'bottom-up' mechanism was adopted by *Varma et al.* [2011] to explain the SWW variability where TSI variations influence the climate mainly through shortwave absorption by the surface [cf. *Meehl et al.*, 2009]. The SWW response under this mechanism is mainly driven by surface temperature gradients and thus does not include any effect of the stratosphere and its ozone content. However, the conversion of enhanced solar ultraviolet (UV) radiation into heat through the Chapman (ozone-oxygen) cycle results in increasing stratospheric temperatures [*Chapman*, 1930]. Moreover, solar variations can affect the stratospheric ozone concentration through modification of photo-dissociation rates. This may have implications for the tropospheric climate response to solar forcing, as the dynamical coupling between the stratosphere and troposphere may substantially influence the surface climate [e.g., *Haigh*, 1996; *Haigh et al.*, 2005; *Meehl et al.*, 2009; *Gray et al.*, 2010; *Bal et al.*, 2011].

[4] A period of special interest regarding the influence of solar variability on Earth's climate is the Maunder Minimum (1645–1715 AD; hereafter MM), which witnessed an unusually low solar output for a relatively long time [*Lean et al.*, 1995]. *Shindell et al.* [2001] discussed the effect of reduced MM solar forcing and stratosphere-troposphere interactions on regional Northern Hemisphere winter climate with a particular eye towards the behaviour of the Arctic Oscillation/North Atlantic Oscillation (AO/NAO). A shift towards the negative phase of the AO/NAO, characterized by weakened Northern Hemisphere westerlies, as suggested by *Shindell et al.* [2001] for the MM was also supported by data and other model studies [e.g., *Langematz et al.*, 2005; *Gray et al.*, 2010; *Spangehl et al.*, 2010].

[5] While most studies on the impact of MM solar forcing on climate focused on the Northern Hemisphere extratropics, the SH climate during MM has received only little attention, even though there is evidence for a solar influence on the SWW and the Antarctic Oscillation (AAO) based on observational data from the past ~50 years [*Roscoe and Haigh*, 2007] and modeling studies [*Haigh*, 1996; *Bal et al.*, 2011]. Here, we will compare two distinct climatic phases in the SH that are characterised by prolonged low and high solar activity, respectively. These two time periods are the Late Maunder Minimum or LMM (1675–1715 AD) and an interval of high solar output just prior to the industrial era, which we simply refer to as the pre-industrial or PI (1716–1790 AD) following the notation by *Spangehl et al.* [2010]. The response of the SWW to changes in solar activity and the role of stratospheric ozone variations during these two time periods is studied using transient climate simulations from the coupled atmosphere-ocean general

[1]MARUM–Center for Marine Environmental Sciences, University of Bremen, Bremen, Germany.
[2]Faculty of Geosciences, University of Bremen, Bremen, Germany.
[3]Institut für Meteorologie, Freie Universität Berlin, Berlin, Germany.
[4]Deutscher Wetterdienst, Offenbach am Main, Germany.
[5]Alfred Wegener Institute for Polar and Marine Research, Bremerhaven, Germany.

Corresponding author: V. Varma, MARUM–Center for Marine Environmental Sciences, University of Bremen, DE-28359 Bremen, Germany. (vvarma@marum.de)

0094-8276/12/2012GL053403

circulation model EGMAM (ECHO-G with Middle Atmosphere Model), carried out by *Spangehl et al.* [2010].

2. Method

[6] The coupled climate model EGMAM [*Huebener et al.*, 2007] is based on ECHO-G [*Legutke and Voss*, 1999]. The atmospheric component is ECHAM4 [*Roeckner et al.*, 1996], extended vertically for the middle atmosphere, with a resolution of T30/L39 ($\sim$3.75° spatial resolution and 39 levels in vertical with 0.01 hPa being the top-most level). The oceanic component is HOPE-G (Hamburg Ocean Primitive Equation Global Model) which includes a dynamic-thermodynamic sea-ice model [*Wolff et al.*, 1997]. The ocean model grid has a horizontal resolution of 2.8° and 20 levels in the vertical (with increased meridional resolution of 0.5° in the tropics).

[7] *Spangehl et al.* [2010] carried out two transient simulations using EGMAM covering the time period of 1630–2000 AD, which were driven by time-dependent changes in radiative forcing accounting for solar variability and volcanic activity [*Crowley*, 2000] as well as changes in greenhouse gas concentrations [*Blunier et al.*, 1995; *Etheridge et al.*, 1996]. The change in TSI from the LMM to the present day is $\sim$0.3% (scaled after *Lean et al.* [1995]). However, it should be noted that the long-term TSI estimates are still subject to uncertainty and discussions [e.g., *Lockwood*, 2011]. The first simulation (hereafter EGMAM1) uses fixed prescribed climatological ozone representing annual cycle variations only [*Brühl*, 1993]. The second simulation (hereafter EGMAM2) additionally includes prescribed variations in stratospheric ozone as part of the solar impact. Here, temporal changes in stratospheric ozone concentration and corresponding changes in stratospheric heating rates due to solar variations are implemented by globally scaling the monthly ozone anomaly fields with TSI variations. The effect of reduced photolytic ozone production on stratospheric ozone concentration during the MM is estimated on the basis of offline calculations [*Langematz et al.*, 2005; *Spangehl et al.*, 2010]. We note that the ozone climatology used here as a background has been corrected for anthropogenic influence and thus represents pre-industrial conditions. Both EGMAM1 and EGMAM2 use a simplified radiation scheme, i.e., the solar spectrum is represented by only two intervals, one for UV/visible (0.2–0.68 μm) and one for near-infrared (0.68–4.0 μm) [*Roeckner et al.*, 1996]. In reality, solar variability is strongly wavelength-dependent, with higher variability in the UV. Therefore, the effect of UV variations on stratospheric heating rates tends to be underestimated within this radiation scheme. We point out, however, that uncertainties in spectral irradiance variability are huge [e.g., *Harder et al.*, 2009; *Haigh et al.*, 2010].

[8] The periods of our interest are LMM and PI as described earlier and the difference in the solar radiative forcing between these two periods is $\sim$0.33 W/m^2 (assuming a planetary albedo of 0.3), i.e. $\sim$0.14% of the total irradiance, while that of volcanic forcing is only $\sim$0.12 W/m^2 [*Spangehl et al.*, 2010, Figure 1a]. Therefore, the dominant forcing of the LMM climate, when compared to PI, is solar. The LMM anomaly of annual-mean stratospheric ozone concentration relative to PI exhibits a reduction of up to $\sim$2%. Both simulations, EGMAM1 and EGMAM2, are started from the same initial conditions taken from a long pre-industrial control run. A more detailed description of the model setup, initialisation and forcings is given in *Spangehl et al.* [2010]. For the following analysis of the climatic response to the applied forcing, temporal means of the entire LMM interval (1675–1715 AD) are compared to averages over the PI interval (1716–1790 AD).

3. Results

[9] The annual-mean zonal wind anomalies along with the vertical velocity anomalies for the period of the LMM relative to the PI are shown in Figure 1 for both EGMAM1 and EGMAM2. At the surface, an overall weakening of the westerlies in the latitude belt between $\sim$40°S and 60°S is found during the LMM (Figures 1a and 1d). North of 40°S, at the northern margin of the SWW belt, a strengthening of the westerlies is found during the LMM in the EGMAM2 experiment. This pattern of SWW weakening between $\sim$40°S and 60°S along with positive westerly wind anomalies to the north of it can be interpreted as an equatorward shift of the annual-mean SWW for the period of lower solar activity. The general SWW weakening during the LMM is also observed in the higher levels of the atmosphere (Figures 1b and 1e). While the weakening observed is statistically significant at the 0.05 level in the experiment with varying solar-induced stratospheric ozone (EGMAM2), it is hardly significant in the experiment with constant ozone (EGMAM1). The austral summer season (December/January/February) witnesses the strongest response pattern of equatorward shift of the SWW in both the simulations (not shown). The low-level zonal wind anomaly at 50°S during the austral summer is about 1 m/s in EGMAM2 (not shown), which is roughly 30% of the zonal wind anomaly found between pre-ozone-hole (1960 AD) and modern ozone-hole eras [*Polvani et al.*, 2011]. The equatorward shift of the annual-mean SWW resembles the negative phase of the AAO [e.g., *Thompson and Wallace*, 2000]. Consistent with the responses in zonal velocity, anomalies in zonally averaged annual-mean vertical velocity (omega) are significant at the 0.05 level only in EGMAM2 (Figures 1c and 1f). For the LMM, EGMAM2 simulates an anomalous ascent around $\sim$40°S and an anomalous descent around $\sim$20°S, indicating a contraction of the Hadley cell.

[10] The LMM annual-mean temperature anomalies relative to the PI are shown in Figure 2. Both simulations, EGMAM1 and EGMAM2, reveal a significant surface temperature cooling in most areas of the SH of similar magnitude. In the tropics, cooler sea surface temperatures lead to reduced latent heat release by moist convection and, hence, cooling of the tropical troposphere in both simulations (Figures 2b and 2d). At higher atmospheric levels, the temperature response in EGMAM2 is much more pronounced (and statistically significant) than in EGMAM1. Here, the dominant feature observed for the LMM temperature anomaly is a general cooling of the lower tropical and subtropical stratosphere that is strongly amplified by the stratospheric ozone loss in EGMAM2 (Figure 2d). Even though there is also a weak cooling of the high-latitude lower stratosphere, effectively, there is a decrease in the meridional stratospheric temperature gradient consistent with a deceleration of the winds according to the thermal wind balance (Figure 1).

4. Discussion

[11] In contrast to EGMAM2, both low-latitude stratospheric temperature and mid-latitude zonal wind anomalies

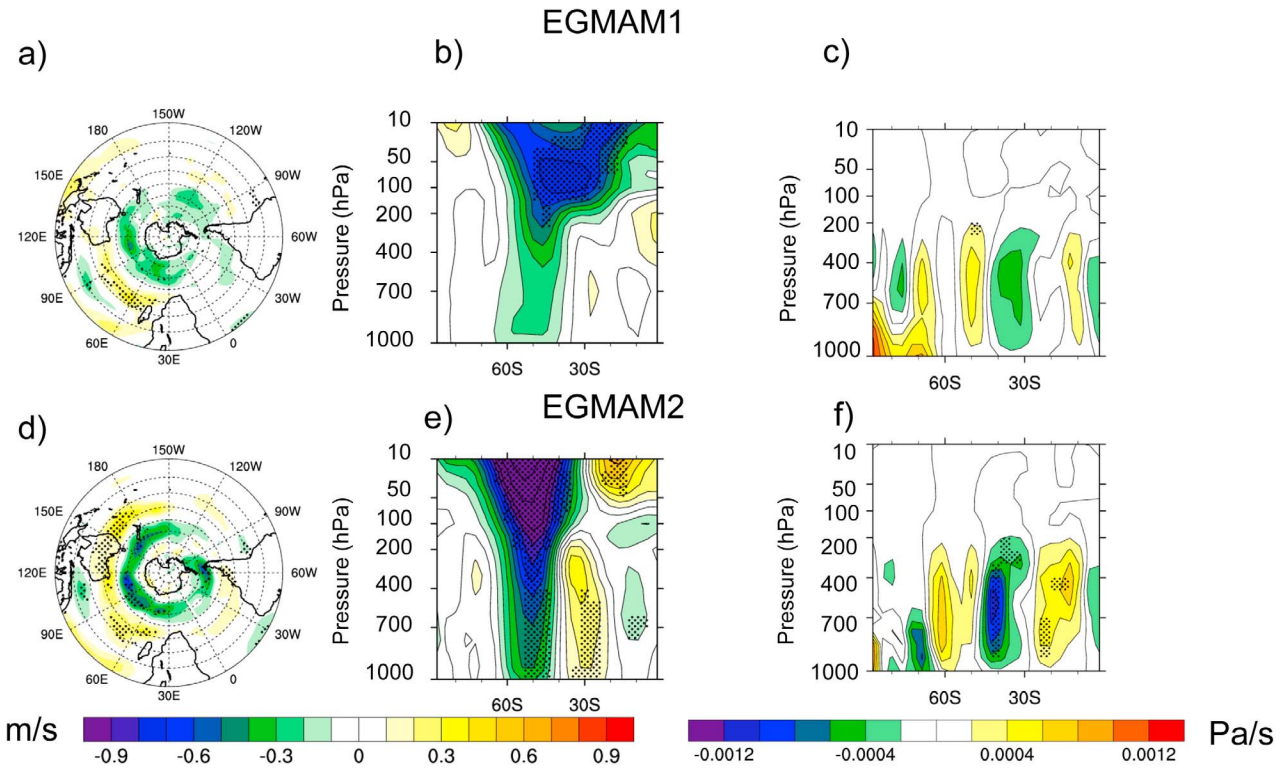

Figure 1. Annual-mean zonal wind and vertical velocity (omega) anomalies (LMM-mean minus PI-mean) in the EGMAM simulations. (a and d) Zonal wind anomalies at 10 m height in EGMAM1 (fixed ozone) and EGMAM2 (varying ozone), respectively. Latitudes are marked from equator to 90°S and are placed at 10° interval. (b and e) Zonally averaged zonal wind anomalies in the Southern Hemisphere in EGMAM1 and EGMAM2, respectively. (c and f) Zonally averaged vertical velocity anomalies in the Southern Hemisphere in EGMAM1 and EGMAM2, respectively. Stippling indicates significance of the anomaly at the 0.05 level according to a Student's t-test.

for the LMM are weak in EGMAM1, suggesting that solar-induced stratospheric ozone variations play a crucial role in governing the SWW response to solar forcing brought about by the dynamical coupling between stratosphere and troposphere. In order to isolate the influence of solar-induced varying ozone on the temperature anomalies, the difference between the annual-mean zonally averaged temperature anomalies between EGMAM2 and EGMAM1 is calculated (Figure 3). The noticeable features of temperature anomalies are the weaker cooling in EGMAM2 compared to EGMAM1 in the SH high-latitude troposphere and lower stratosphere along with a stronger cooling in the SH mid-to-low latitudes lower stratosphere. In both the simulations, the stratospheric warming in the high-latitudes is not statistically significant (from Figures 2b and 2d) and hence is not further discussed. The relative tropospheric warming in high latitudes is consistent with the negative polarity of the AAO associated with the weaker and equatorward shifted SWW in the EGMAM2 simulation [e.g., *Thompson and Wallace*, 2000]. In the experiment with solar-induced varying stratospheric ozone, the simulated year-round cooling of the low-latitude lower stratosphere during solar minima is consistent with the stratospheric response to the 11-year Sunspot cycle based on observations and re-analysis data, whereas the observed correlation between solar flux and stratospheric temperatures is ambiguous in high latitudes [*Labitzke*, 2001].

[12] Potential mechanisms by which stratospheric ozone and temperature anomalies may affect the troposphere are still unclear and have been rigorously discussed [e.g. *Shepherd*, 2002; *Haynes*, 2005; *Simpson et al.*, 2009; *Thompson et al.*, 2011]. However, results obtained with a simplified model of the general atmospheric circulation by *Haigh et al.* [2005] and *Simpson et al.* [2009] show striking similarities with the response found in EGMAM2. According to *Haigh et al.* [2005], low-latitude cooling of the lower stratosphere decreases the static stability in this region, raises the tropopause and enhances the wave fluxes there, thus leading to coherent changes through the depth of the troposphere, involving a contraction of the Hadley cell and an equatorward shift of the westerlies. *Simpson et al.* [2009] demonstrated how thermal perturbations in the tropical lower stratosphere create horizontal eddy momentum and heat flux anomalies through their influence on vertical and meridional temperature gradients around the tropopause region. Internal feedbacks involving changes in tropospheric eddy momentum fluxes are required to produce the full response in zonal wind shift [*Kushner and Polvani*, 2004; *Simpson et al.*, 2009].

[13] Our model evidence for a possible relation between solar activity and SWW shifts is supported by proxy data. A high-accumulation rate marine sediment core (GeoB3313-1) from the Chilean continental slope (41°S, 74.45°W) is interpreted as a Holocene record of local rainfall variations through

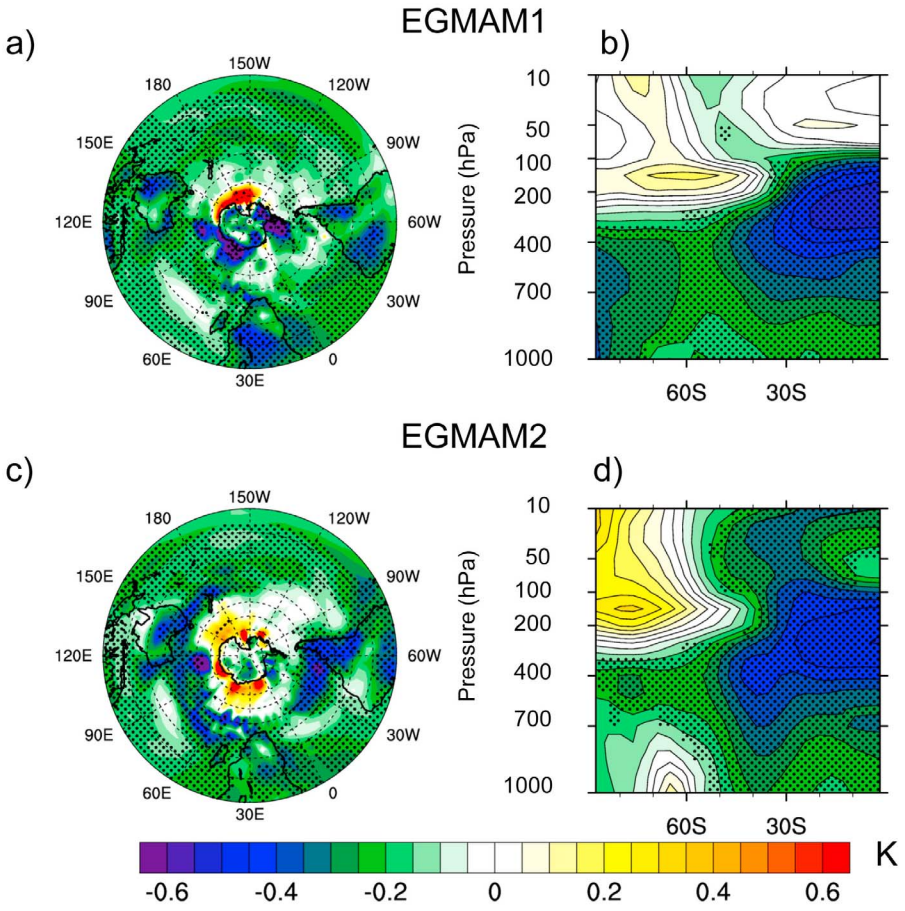

Figure 2. Annual-mean temperature anomalies (LMM-mean minus PI-mean) in the EGMAM simulations. (a and c) Surface temperature anomalies in EGMAM1 (fixed ozone) and EGMAM2 (varying ozone), respectively. Latitudes are marked from equator to 90°S and are placed at 10° interval. (b and d) Zonally averaged temperature anomalies in the Southern Hemisphere in EGMAM1 and EGMAM2, respectively. Stippling indicates significance of the anomaly at the 0.05 level according to a Student's t-test.

its iron content, which can be interpreted in terms of SWW position [*Lamy et al.*, 2001; *Varma et al.*, 2011]. A comparison of this iron record with reconstructions of solar activity based on ^{14}C [*Solanki et al.*, 2004] and ^{10}Be [*Steinhilber et al.*, 2009] for the last 500 years, which include the Dalton Minimum (ca. 1795–1825 AD) and the MM, is shown in Figure 4. A higher concentration of iron in the sediment core indicates drier conditions probably due to southward shifted SWW, whereas a lower iron concentration is indicative of wetter conditions suggesting northward shifted SWW [*Lamy et al.*, 2001]. During the solar minimum periods (e.g. Dalton Minimum and MM), the iron record shows negative anomalies suggesting an enhanced precipitation in the hinterland of the coring site. Pearson correlation coefficients suggest a statistically significant link between solar activity and the SWW, characterized by an equatorward (poleward) shift of the SWW during periods of lower (higher) solar activity, which is especially pronounced during the MM (Figure 4).

[14] Since a low resolution model has been used in this study, local features and in particular, orographic rainfall at the Andes cannot be fully captured. However, EGMAM still simulates positive precipitation anomalies over the region of

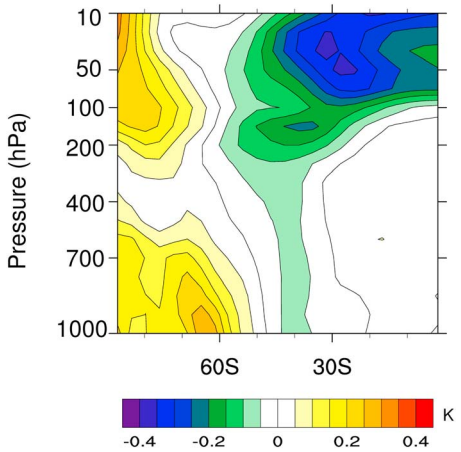

Figure 3. Difference between the zonally averaged annual-mean temperature anomalies (LMM-mean minus PI-mean) in EGMAM2 and EGMAM1 simulations (i.e., 'Figure 2d minus Figure 2b') in the Southern Hemisphere.

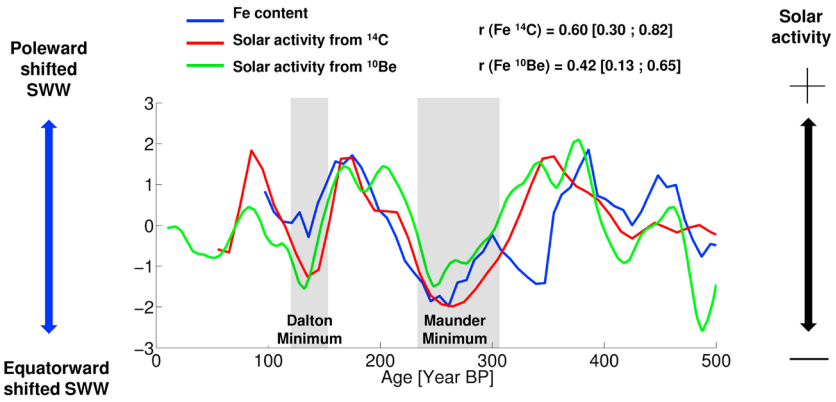

Figure 4. Reconstruction of the SWW position (blue line, based on the GeoB3313-1 iron record [*Lamy et al.*, 2001]) versus solar activity based on ^{10}Be (green line [*Steinhilber et al.*, 2009]) and ^{14}C (red line [*Solanki et al.*, 2004]), for the last 500 years. Grey bars mark the low solar activity periods of the Dalton Minimum and the Maunder Minimum. Time series are unsmoothed, detrended and standardized. The negative (positive) iron anomalies suggest northward (southward) shifted SWW [*Lamy et al.*, 2001; *Varma et al.*, 2011]. 95% confidence intervals (in brackets) for Pearson correlation coefficients (r) were calculated using a bootstrap method, where autocorrelation has been taken into account [*Mudelsee*, 2003].

enhanced westerlies in Patagonia (in particular during austral summer), but statistically not significant at the 0.05 significance level according to a t-test (not shown).

5. Conclusions

[15] We studied the stratospheric influence on the variability of the SWW during the period from LMM to PI, using results from a coupled atmosphere-ocean model with a detailed representation of the middle atmosphere. The analysis of two transient simulations with fixed as well as solar-induced varying stratospheric ozone points to an important effect of solar-induced stratospheric ozone variations on the SWW during the MM and possibly also during other multi-decadal to centennial solar minima. The model results support the hypothesis that during periods of lower solar output, the annual-mean SWW tend to get weaker on the poleward side and exhibit an equatorward shift. In addition, proxy evidence was presented, which supports the hypothesis of an equatorward SWW shift during solar minima.

[16] While a 'bottom-up' mechanism via shortwave absorption at the surface in combination with feedbacks involving ocean and sea-ice dynamics was suggested by *Varma et al.* [2011] to explain the SWW response to centennial-scale changes in TSI during the Late Holocene, the present study highlights the significance of the stratosphere along with its ozone content as a potential driver for multi-decadal to centennial-scale extratropical climate variability in the Southern Hemisphere, through a 'top-down' process. Amplification of the solar signal in low-latitude stratospheric temperature by changes in photochemical net ozone production and associated heating rates appears to be crucial in this process. We propose that the 'bottom-up' and 'top-down' mechanisms are not mutually exclusive and that the processes linking solar variability to the SWW in the two different ways may complement each other, thus leading to a stronger total response than given by each individual process alone.

[17] We finally conclude that the role of the Sun in driving SH extratropical climate dynamics has likely been underestimated in previous simulations of past climate change, using models that did not account for solar-induced stratospheric ozone variations. Future studies should further evaluate the uncertainty range of past tropospheric and stratospheric responses to solar forcing by using different reconstructions of total and spectral solar irradiance as well as implementing interactive climate-chemistry feedbacks.

[18] **Acknowledgments.** This work is the outcome of a research stay (by Vidya Varma) at the Institut für Meteorologie (Freie Universität Berlin, Germany). The study was funded through the DFG Priority Programme "INTERDYNAMIK". We acknowledge the use of the NCAR Command Language (NCL) in our data analysis and visualization.

[19] The Editor and authors thank two anonymous reviewers for assistance evaluating this paper.

References

Anderson, R. F., S. Ali, L. I. Bradtmiller, S. H. H. Nielsen, M. Q. Fleischer, B. E. Anderson, and L. H. Burckle (2009), Wind-driven upwelling in the Southern Ocean and the deglacial rise in atmospheric CO_2, *Science*, *323*, 1443–1448, doi:10.1126/science.1167441.

Bal, S., S. Schimanke, T. Spangehl, and U. Cubasch (2011), On the robustness of the solar cycle signal in the Pacific region, *Geophys. Res. Lett.*, *38*, L14809, doi:10.1029/2011GL047964.

Biastoch, A., C. W. Böning, F. U. Schwarzkopf, and J. R. E. Lutjeharms (2009), Increase in Agulhas leakage due to poleward shift of Southern Hemisphere westerlies, *Nature*, *462*, 495–498, doi:10.1038/nature08519.

Blunier, T., J. Chappellaz, J. Schwander, B. Stauffer, and D. Raynaud (1995), Variations in atmospheric methane concentration during the Holocene epoch, *Nature*, *374*, 46–49, doi:10.1038/374046a0.

Brühl, C. (1993), Atmospheric effects of stratospheric aircraft: Report of the 1992 Models and Measurements Workshop, *NASA Ref. Publ.*, *1292II*, 240 pp.

Chapman, S. (1930), A theory of upper-atmospheric ozone, *Memoirs of the Royal Meteorological Society*, *3*(26), 103–125.

Crowley, T. J. (2000), Causes of climate change over the past 1000 years, *Science*, *289*, 270–277, doi:10.1126/science.289.5477.270.

Etheridge, D. M., L. P. Steele, R. L. Langenfelds, R. J. Francey, J.-M. Barnola, and V. I. Morgan (1996), Natural and anthropogenic changes in atmospheric CO_2 over the last 1000 years from air in Antarctic ice and firn, *J. Geophys. Res.*, *101*, 4115–4128, doi:10.1029/95JD03410.

Gray, L. J., et al. (2010), Solar influences on climate, *Rev. Geophys.*, *48*, RG4001, doi:10.1029/2009RG000282.

Haigh, J. D. (1996), The impact of solar variability on climate, *Science*, *272*, 981–984, doi:10.1126/science.272.5264.981.

Haigh, J. D., M. Blackburn, and R. Day (2005), The response of tropospheric circulation to perturbations in lower-stratospheric temperature, *J. Clim.*, *18*, 3672–3685, doi:10.1175/JCLI3472.1.

Haigh, J. D., A. R. Winning, R. Toumi, and J. W. Harder (2010), An influence of solar spectral variations on radiative forcing of climate, *Nature*, *467*, 696–699, doi:10.1038/nature09426.

Harder, J. W., J. M. Fontenla, P. Pilewskie, E. C. Richard, and T. N. Woods (2009), Trends in solar spectral irradiance variability in the visible and infrared, *Geophys. Res. Lett.*, *36*, L07801, doi:10.1029/2008GL036797.

Haynes, P. (2005), Stratospheric dynamics, *Annu. Rev. Fluid Mech.*, *37*, 263–293, doi:10.1146/annurev.fluid.37.061903.175710.

Huebener, H., U. Cubasch, U. Langematz, T. Spangehl, F. Nierhorster, I. Fast, and M. Kunze (2007), Ensemble climate simulations using a fully coupled ocean-troposphere-stratosphere general circulation model, *Philos. Trans. R. Soc. A*, *365*, 2089–2101, doi:10.1098/rsta.2007.2078.

Kushner, P. J., and L. M. Polvani (2004), Stratosphere-troposphere coupling in a relatively simple AGCM: The role of eddies, *J. Clim.*, *17*, 629–639, doi:10.1175/1520-0442(2004)017<0629:SCIARS>2.0.CO;2.

Labitzke, K. (2001), The global signal of the 11-year sunspot cycle in the stratosphere: Differences between solar maxima and minima, *Meteorol. Z.*, *10*, 83–90, doi:10.1127/0941-2948/2001/0010-0083.

Lamy, F., D. Hebbeln, U. Röhl, and G. Wefer (2001), Holocene rainfall variability in southern Chile: A marine record of latitudinal shifts of the southern westerlies, *Earth Planet. Sci. Lett.*, *185*, 369–382, doi:10.1016/S0012-821X(00)00381-2.

Langematz, U., A. Claussnitzer, K. Matthes, and M. Kunze (2005), The climate during the Maunder Minimum: A simulation with the Freie Universität Berlin Climate Middle Atmosphere Model (FUB-CMAM), *J. Atmos. Sol. Terr. Phys.*, *67*, 55–69, doi:10.1016/j.jastp.2004.07.017.

Lean, J., J. Beer, and R. Bradley (1995), Reconstruction of solar irradiance since 1610: Implications for climate change, *Geophys. Res. Lett.*, *22*, 3195–3198, doi:10.1029/95GL03093.

Legutke, S., and R. Voss (1999), The Hamburg Atmosphere-Ocean Coupled Circulation Model ECHO-G, *Tech. Rep. 18*, Dtsch. Klimarechenzent., Hamburg, Germany.

Lockwood, M. (2011), Shining a light on solar impacts, *Nat. Clim. Change*, *1*, 98–99, doi:10.1038/nclimate1096.

Meehl, G. A., J. M. Arblaster, K. Matthes, F. Sassi, and H. van Loon (2009), Amplifying the Pacific climate system response to a small 11 year solar cycle forcing, *Science*, *325*, 1114–1118, doi:10.1126/science.1172872.

Mudelsee, M. (2003), Estimating Pearson's correlation coefficient with bootstrap confidence interval from serially dependent time series, *Math. Geol.*, *35*, 651–665, doi:10.1023/B:MATG.0000002982.52104.02.

Polvani, L. M., D. W. Waugh, G. J. P. Correa, and S. W. Son (2011), Stratospheric ozone depletion: The main driver of 20th century atmospheric circulation changes in the Southern Hemisphere, *J. Clim.*, *24*, 795–812, doi:10.1175/2010JCLI3772.1.

Roeckner, E., K. Arpe, L. Bengtsson, M. Christoph, M. Claussen, L. Dümenil, M. Esch, M. Giorgetta, U. Schlese, and U. Schulzweida (1996), The atmospheric general circulation model ECHAM-4: Model description and simulation of present-day climate, *Rep. 218*, Max Planck Inst. für Meteorol., Hamburg, Germany.

Roscoe, H. K., and J. D. Haigh (2007), Influences of ozone depletion, the solar cycle and the QBO on the Southern Annular Mode, *Q. J. R. Meteorol. Soc.*, *133*, 1855–1864, doi:10.1002/qj.153.

Shepherd, T. G. (2002), Issues in stratosphere-troposphere coupling, *J. Meteorol. Soc. Jpn.*, *80*, 769–792, doi:10.2151/jmsj.80.769.

Shindell, D. T., G. A. Schmidt, M. E. Mann, D. Rind, and A. Waple (2001), Solar forcing of regional climate change during the Maunder Minimum, *Science*, *294*, 2149–2152, doi:10.1126/science.1064363.

Shulmeister, J., et al. (2004), The Southern Hemisphere westerlies in the Australasian sector over the last glacial cycle: A synthesis, *Quat. Int.*, *118-119*, 23–53, doi:10.1016/S1040-6182(03)00129-0.

Simpson, I. R., M. Blackburn, and J. D. Haigh (2009), The role of eddies in driving the tropospheric response to stratospheric heating perturbations, *J. Atmos. Sci.*, *66*, 1347–1365, doi:10.1175/2008JAS2758.1.

Solanki, S. K., I. G. Usoskin, B. Kromer, M. Schüssler, and J. Beer (2004), Unusual activity of the Sun during recent decades compared to the previous 11,000 years, *Nature*, *431*, 1084–1087, doi:10.1038/nature02995.

Spangehl, T., U. Cubasch, C. C. Raible, S. Schimanke, J. Körper, and D. Hofer (2010), Transient climate simulations from the Maunder Minimum to present day: Role of the stratosphere, *J. Geophys. Res.*, *115*, D00I10, doi:10.1029/2009JD012358. [Printed *116*(D1), 2011.]

Steinhilber, F., J. Beer, and C. Fröhlich (2009), Total solar irradiance during the Holocene, *Geophys. Res. Lett.*, *36*, L19704, doi:10.1029/2009GL040142.

Thompson, D. W. J., and J. M. Wallace (2000), Annular modes in the extratropical circulation. Part I: Month-to-month variability, *J. Clim.*, *13*, 1000–1016, doi:10.1175/1520-0442(2000)013<1000:AMITEC>2.0.CO;2.

Thompson, D. W. J., S. Solomon, P. J. Kushner, M. H. England, K. M. Grise, and D. J. Karoly (2011), Signatures of the Antarctic ozone hole in Southern Hemisphere surface climate change, *Nat. Geosci.*, *4*, 741–749, doi:10.1038/ngeo1296.

Toggweiler, J. R., and B. Samuels (1995), Effect of Drake Passage on the global thermohaline circulation, *Deep Sea Res., Part I*, *42*, 477–500, doi:10.1016/0967-0637(95)00012-U.

Toggweiler, J. R., J. L. Russell, and S. R. Carson (2006), Midlatitude westerlies, atmospheric CO_2, and climate change during the ice ages, *Paleoceanography*, *21*, PA2005, doi:10.1029/2005PA001154.

Varma, V., M. Prange, F. Lamy, U. Merkel, and M. Schulz (2011), Solar-forced shifts of the Southern Hemisphere westerlies during the Holocene, *Clim. Past.*, *7*, 339–347, doi:10.5194/cp-7-339-2011.

Wolff, J., E. Maier-Reimer, and S. Legutke (1997), The Hamburg primitive equation model HOPE, *Tech. Rep. 18.*, Dtsch. Klimarechenzent., Hamburg, Germany.